A Robust Waveguide Millimeter-Wave Noise Source

Negar Ehsan*, Jeffrey Piepmeier*, Michael Solly*, Shawn Macmurphy†, Jared Lucey*, and Edward Wollack*
*NASA Goddard Space Flight Center
Greenbelt, Maryland 20771
†AS and D, Inc.
Greenbelt, Maryland 20771
E-mail: negar.ehsan@nasa.gov

***Abstract*—This paper presents the design, fabrication, and characterization of a millimeter-wave noise source for the 160–210 GHz frequency range. The noise source has been implemented in an E-split-block waveguide package and the internal circuitry was developed on a quartz substrate. The measured excess noise ratio at 200 GHz is 9.6 dB.**

I. Introduction

Millimeter- and submillimeter-wave remote sensing has applications in atmospheric sounding, precipitation, and ice cloud measurements [1]. G-band (160–210 GHz), due to the water vapor absorption line around 183 GHz, is one of the widely-used channels for atmospheric sciences and weather forecasting. In the past decades extensive research has been performed to develop receiver components at mm- and submm-wave frequencies, such as low-noise amplifiers, local oscillators, mixers, etc. [2], [3]. Corresponding advances in integrated noise sources have largely been absent. For passive mm-wave remote sensing applications, the availability of such a noise source would clearly provide an enabling technology for NASA's envisioned Venture-class Earth science missions. A noise source enables relative radiant power calibration of the receiver at the sensing frequency, which reduces or eliminates the requirement of a clear view to cold space (reducing instrument mass, cost, and complexity).

In radiometric systems, a typical limiting factor for achieving high radiometric sensitivity is the variation in gain [4]. The Dicke radiometer and variation on this theme provide a path to signal stabilization and calibration by switching the receiver input between a known temperature source and the antenna at a rate above these variations [4], [5]. The known temperature source can either be a passive reference load such as a resistor, an active source such as a noise diode, another antenna looking at a known-temperature blackbody load, or any combination of the above depending on the radiometer architecture [6].

At high frequencies, due to their low junction capacitance, Schottky diodes can be used as noise sources when they are reverse-biased to avalanche breakdown. The noise current arrises from collision-induced ionization via free carriers colliding with and knocking free new carriers in the semiconducting media [7]–[9]. Bowen showed silicon Schottky diodes mounted in a micro-lid package, placed at the terminal of a broadband linearly-tapered slot antenna, can generate 19.8 dB excess noise ratio (ENR) at 40 GHz when reverse-biased to avalanche breakdown [9].

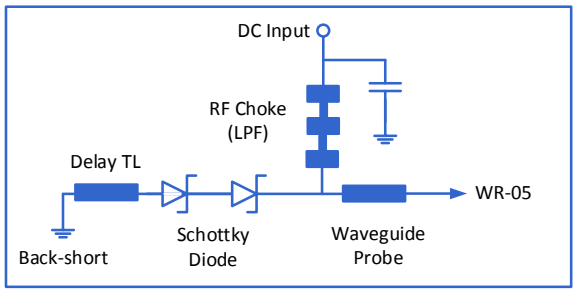

(a)

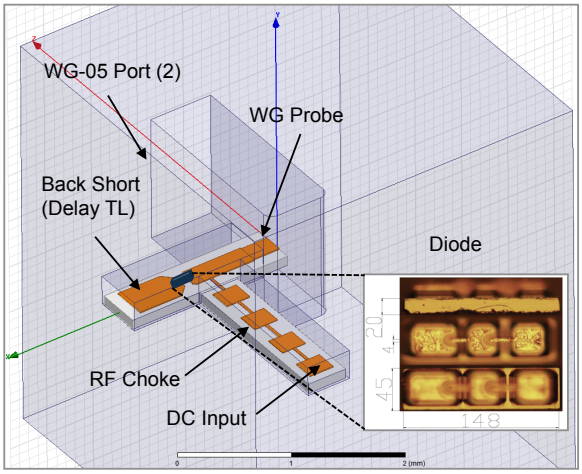

(b)

Fig. 1. a) A block diagram showing the design of the noise source. The main source of the RF noise is a reverse-biased Schottky diode. (b) 3D view of the noise source as simulated in a finite element method electromagnetic modeler. The on-chip circuitry, including the back-short, RF choke, and microstrip-to-waveguide probe are designed on a quartz substrate.

Recently, GaAs Schottky diodes used in frequency mixer and multiplier designs were used to demonstrate a noise source with 8–10 dB ENR at breakdown, when amplitude modulated with reverse bias at both 120 GHz and 200 GHz [10]. However, the device lifetime was short, and a dedicated noise source package was not developed.

In this paper we describe the development of a G-band noise source using GaAs Schottky diodes, implemented in microstrip and waveguide topologies. A foremost goal of this study is

to demonstrate a mm-wave noise source that can be easily integrated with receivers at mm-wave frequencies. This noise source is compatible with chip devices such as couplers or switches, as the circuitry is designed on microstrip; the noise source can operate with continuous power rather than pulsed power, due to the use of heat sinking elements (vias in the back-short), and it is compatible with waveguide components.

II. Noise Source Design and Fabrication

The noise source design consists of a mm-wave noise generator, bias circuitry, an RF back-short, and a waveguide probe. Fig. 1(a) shows a simplified block diagram of the G-band noise source design, and Fig. 1(b) shows the full-wave electromagnetic model of the design. The source of noise in this circuit is a double GaAs Schottky diode (two in series, on one chip) from Virginia Diodes, Inc. (VDI). The inset in Fig. 1(b) shows a photograph of the Schottky diode, which is $148\,\mu\text{m} \times 45\mu\text{m} \times 20\mu\text{m}$. The bias circuitry for the diode was designed in microstrip on a quartz substrate. The bias tee consists of a low-pass filter with an alternating high/low-impedance configuration for blocking RF, and a feed-thru (EMI filter) that connects the filter to bias line with an internal capacitor to short any RF noise coming from the DC path. Due to the frequency of operation the noise source must be designed in a waveguide package. A microstrip-to-waveguide probe transition is designed for the entire WR-5.1 bandwidth, with a longitudinal probe configuration [11]. Fig. 2(a) shows the simulated S-parameters of the microstrip-to-waveguide transition with the RF choke. In this plot, port 1 is the waveguide port and port 2 is a "lumped port" at the input of the diode (the diode is not modeled in this simulation). As shown, the transition has better than 10 dB return loss across the band, and the transmission loss is ≤ 1 dB.

When a Schottky diode is reverse-biased it generates noise waves from both terminals and thus in both directions in the microstrip guide, with 180° phase difference. To direct all of the noise to the desired RF path, an RF short is designed to reflect the noise in the other direction and thus add in phase with the outgoing noise. Fig. 2(b) shows the simulated response of the RF back-short on the Smith chart. The back-short consists of a capacitive delay transmission line with phase delays of 180° at 184 GHz, 160° at 191 GHz, and -160° at 176 GHz. The back-short is designed with multiple vias to aid in heat-sinking the diodes; this feature enables continuous biasing rather than modulated.

An E-plane WR-5.1 split-block waveguide housing was designed for the noise source and fabricated from brass. Fig.3 (a) shows the fabricated package, and Fig. 3 (b) shows the bottom half with the internal components in place.

III. Measured Results

The noise source has been tested for both S-parameter response and noise performance. Since the impedance of the diode is not known, in order to verify the performance of the microstrip-to-waveguide transition on quartz, we designed, fabricated, and packaged a back-to-back structure. A set of

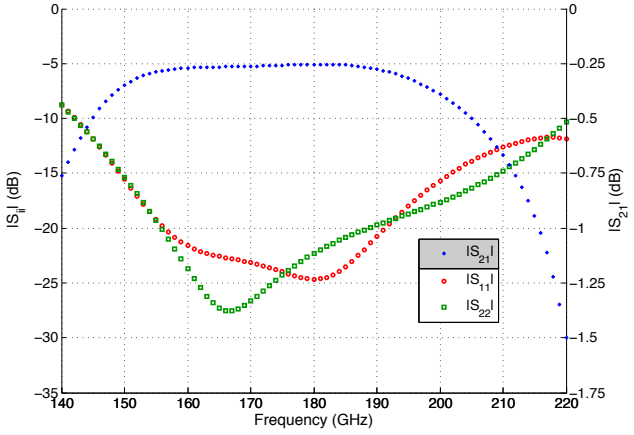

(a)

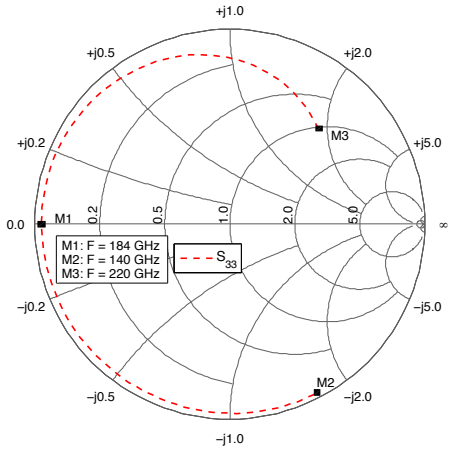

(b)

Fig. 2. (a) Simulated S-parameter results of the probe-to-waveguide transition including the RF filter; port 2 is the waveguide port, and port 1 is a lumped port at input of the diode. (b) Simulated S-parameter results of the back-short shown on the Smith chart. The back-short is 180° at 184 GHz, 160° at 191 GHz, and -160° at 176 GHz.

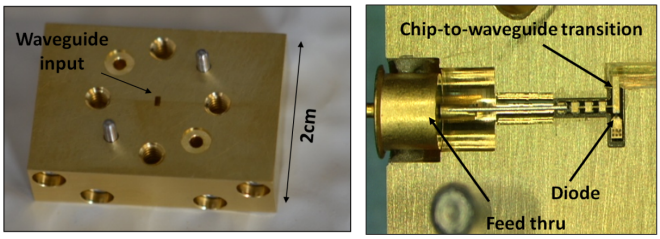

(a) (b)

Fig. 3. (a) A photograph of the packaged noise source; the package is designed around a split-block WR-5.1 waveguide. (b) A photograph of the internal components of the noise source (bottom half of the package).

WR-5.1 extension heads from Oleson Microwave Labs (OML) with an Agilent PNA is used to measure its S-parameters. The extension heads were calibrated using a short, load, offset short, offset load, and thru (SLOSOLT) calibration method. Fig. 4(a) shows the S-parameter response of the simulated and measured back-to-back transition. The measurement and

simulation results agree closely, verifying the performance of the transition from microstrip to waveguide. The measured performance of the transitions in the back-to-back configuration is reduced due to standing waves between the elements [12]. We note that the microstrip-to-waveguide transition's return loss is 10 dB up to 210 GHz as shown in Section II, Fig. 2(a). The packaged noise diode is then tested for S-parameter results. Fig. 4(b) shows the measured $|S_{11}|$ of the noise source. Since the diode impedance was not known, the microstrip components were designed for a $50\,\Omega$ system. It appears the diode is well-matched to $50\,\Omega$ at 200 GHz with -12 dB of return loss. $|S_{11}|$ was measured at bias points from $V_d = -12\,\text{V}$ to $V_d = -16.4\,\text{V}$, and no sensitivity to bias voltage was noted. From the data provided by the vendor, the S-parameter measurement, and reanalysis of the design it is evident that the input impedance of the diode is capacitive with series resistance on the order of $C_j = 12\,\text{fF}$ and $R_s = 50\,\Omega$ to $100\,\Omega$. Further measurement and analysis are required to verify the input impedance of the diode.

To measure the noise performance of the noise source, a G-band receiver was set up and a Y-factor measurement was performed. Fig. 5 shows the block-diagram of the measurement system, which includes a circular G-band horn, an E-plane bend, a 4" waveguide, an 8 dB coupler to couple the noise from the noise source, a second-harmonic mixer from VDI, a $\times 6$ multiplier, a synthesizer, an IF LNA, a bandpass filter centered at 250 MHz with 140 MHz bandwidth, and a power meter. To perform the Y-factor measurement we used two targets: one at 77 K and the other at room temperature. A measurement was performed for two cases at each frequency: the diode off and the diode on. For the "on" state the diode was reverse-biased at $V_d = 16.39\,\text{V}$ and $I_d = 6\,\text{mA}$. The synthesizer frequency was swept to measure the noise at different frequencies. All the front-end losses (waveguide E-plane bend, transmission lines, and the coupler) were measured as an assembly using the OML extension heads and the PNA, and used to correct the response. The following equations show the calculations that were used to extract the excess noise ratio (ENR) from the measurements:

$$Y_{\text{on}} = \frac{P_{\text{onHot}}}{P_{\text{onCold}}} \tag{1}$$

$$Y_{\text{off}} = \frac{P_{\text{offHot}}}{P_{\text{offCold}}} \tag{2}$$

$$T_{\text{on}} = \frac{T_{\text{Hot}} - Y_{\text{on}} \times T_{\text{Cold}}}{Y_{\text{on}} - 1} \tag{3}$$

$$T_{\text{off}} = \frac{T_{\text{Hot}} - Y_{\text{off}} \times T_{\text{Cold}}}{Y_{\text{off}} - 1} \tag{4}$$

$$T_{\text{NS}} = (T_{\text{on}} - T_{\text{off}}) \times C \times \frac{L_2}{L_1} \tag{5}$$

$$\text{ENR} = 10 \log \left(\frac{T_{\text{NS}}}{290} - 1 \right), \tag{6}$$

where P_{onHot} and P_{onCold} are the measured powers with the noise diode on looking at the room temperature target and at the cold target, respectively. P_{offHot} and P_{offCold} are the measured power when the noise diode is off looking at the room temperature target and cold target, respectively. L_1 is the loss from the bend, 4" transmission line between the antenna and the coupler, and the coupler; C is the coupling factor, and L_2 is the loss of the transmission line from the noise source to the coupler.

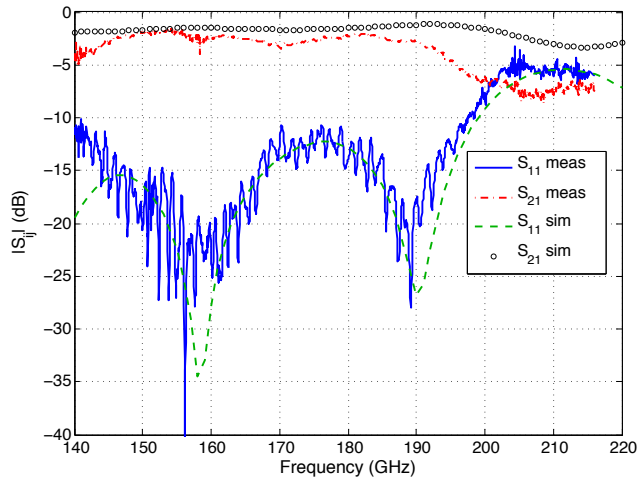

(a)

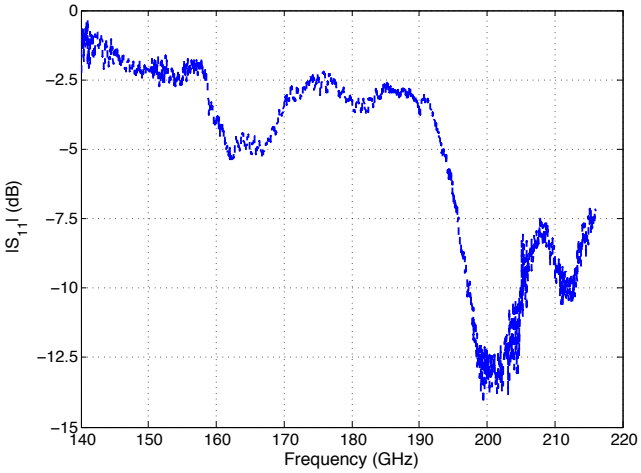

(b)

Fig. 4. (a) Measured S-parameter results of a back-to-back microstrip-to-waveguide transition; an existing package was used to verify the performance of the transition. (b) Measured $|S_{11}|$ of the packaged noise source; the input impedance of the diode is not known and the circuitry was designed to match $50\,\Omega$.

Fig. 6 shows the calculated ENR of the G-band noise source as a function of frequency based on the measured results. The packaged noise source generates approximately 10 dB ENR at 200 GHz. This result is consistent with the return loss measurement shown in Fig. 4(b), which indicates the return loss is best at 200 GHz. Based on these results, the ENR of the noise source can be improved more than 3 dB by matching to the impedance of the diode at the lower frequencies.

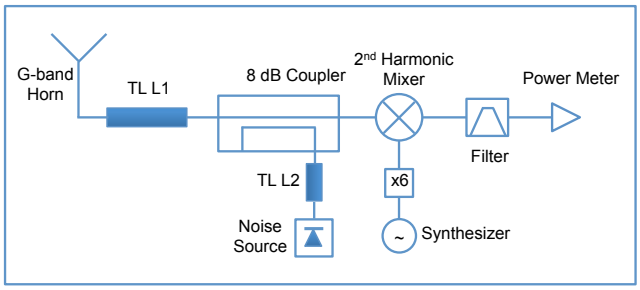

Fig. 5. Block diagram of the measurement setup for characterizing the noise performance of the noise source. The measurement was performed via Y-factor measurements with two targets, one at 77 K, and the other at room temperature.

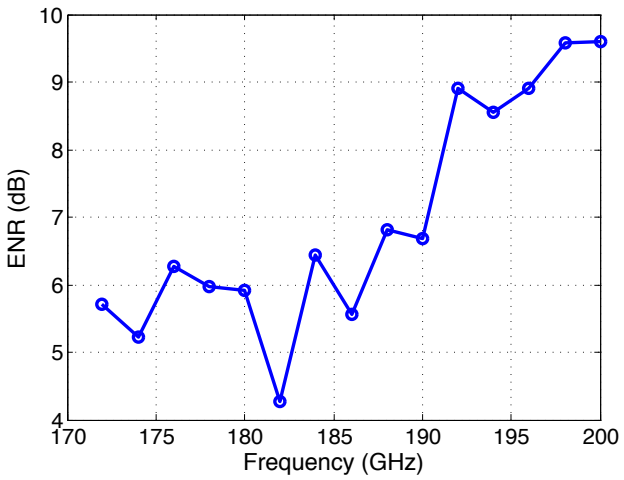

Fig. 6. ENR measurement results, measured via the Y-factor measurement set-up shown in Fig. 5. Front-end components including transmission lines, bends, and coupler, were measured both individually and integrated. The reported response has been corrected for these losses.

IV. Conclusion

In this paper we presented a mm-wave noise source with ENR $\approx$ 10 dB at 200 GHz. The noise source is implemented in microstrip on a quartz substrate embedded into a brass waveguide housing. Based on the measured results, it is possible to further improve the output noise of the component by determining the input impedance of the Schottky diode and designing a broadband matching network. By retuning the circuit response to better match the input impedance of the diode, we believe the output ENR can be increased by 3 dB at the center of the band based on these observations. The noise source, as a calibration source at the front-end of a receiver, is accompanied by either a low-loss coupler and or a low-loss switch. Since the noise source is placed in the system before any amplification stages at the front-end, losses are extremely important. It is highly desirable to next develop an integrated system in which a low-loss coupler or low-loss switch is integrated with the noise source.

Acknowledgment

The authors would like to thank the U.S. Army Research Laboratory and Dr. Charles Dietlein for assistance in characterizing the S-parameter response of the noise source and waveguide components.

References

[1] K.F. Evans, S.J. Walter, A.J. Heymsfield, and G.M. McFarquhar, "Submillimeter-wave cloud ice radiometer: Simulations of retrieval algorithm performance," *J. Geophys. Res.*, vol. 107, no. D3, pp. AAC 2-1–AAC 2-21, February 2002.

[2] P. Kangaslahti, D. Pukala, T. Gaier, W. Deal, X. Mei, and R. Lai, "Low-noise amplifier for 180 GHz frequency band," *IEEE MTT-S International Microwave Symposium Digest*, 2008, pp. 451–454.

[3] D. Pukala, L. Samosa, T. Gaier, A. Fung, X. Mei, W. Yoshida, J. Lee, J. Uyeda, P. Liu, W. Deal, V. Radisic, and R. Lai, "Submillimeter-wave InP MMIC amplifiers from 300–345 GHz," *IEEE Microwave and Wireless Components Letters,* vol. 18, no. 1, pp. 61–63, January 2008.

[4] R.H. Dicke, "The measurement of thermal radiation at microwave frequencies," *Review of Scientific Instruments*, vol. 17, no. 7, pp. 268–275, 1946.

[5] K. Rohlfs, Tools of Radio Astronomy, Berlin and New York, Springer-Verlag, 1986, p. 332, vol. 1, 1986.

[6] F. Ulaby, R. Moore, and A. Fung, *Microwave Remote Sensing, Active And Passive, Volume 1, Microwave Remote Sensing Fundamentals and Radiometry*, Norwood, MA: Artech House 1981, p. 377.

[7] R.H. Haitz and F.L. Opp, "A solid state broadband microwave noise source," *International Electron Devices Meeting*, vol. 14, p. 46, 1968.

[8] R.H. Haitz and F.W. Voltmer, "Noise of a self-sustaining avalanche discharge in silicon: Studies at microwave frequencies," *J. Appl. Phys.*, vol. 39, no. 7, pp. 3379–3384, June 1968.

[9] J.W. Bowen, "A solid-state noise source for millimeter wave spectrometry," *J. Infrared and Millimeter Waves*, vol. 17, no. 3, 1996.

[10] J. Hesler, "Active Noise Sources," Virginia Diodes Inc., Charlottesville, VA, SBIR Phase I Rep. NNX09CD42P, July 2009.

[11] Y. Leong and S. Weinreb, "Full band waveguide-to-microstrip probe transition," *Microwave Symposium Digest, IEEE MTT-S International*, vol. 4, pp. 1435–1438, June 1999.

[12] E.J. Wollack and F.M. Vanin, "Broadband Transitions for Micromachined Waveguides," *Microwave Symposium Digest, IEEE MTT-S International,* pp. 1749–1752, June 2007.